Folate receptor-β imaging using 99mTc-folate to explore distribution of polarized macrophage populations in human atherosclerotic plaque

Jager, Nynke A.; Westra, Johanna; Golestani, Reza; van Dam, Gooitzen; Low, Philip S.; Tio, Rene A.; Slart, Riemer; Boersma, Hendrikus; Bijl, Marc; Zeebregts, Johannes

Published in:
Journal of Nuclear Medicine

DOI:
10.2967/jnumed.114.143180

Publication date:
2014

Folate Receptor-β Imaging Using ^{99m}Tc-Folate to Explore Distribution of Polarized Macrophage Populations in Human Atherosclerotic Plaque

Nynke A. Jager[1,2], Johanna Westra[2], Reza Golestani[3], Gooitzen M. van Dam[1], Philip S. Low[4], René A. Tio[5], Riemer H.J.A. Slart[6], Hendrikus H. Boersma[6,7], Marc Bijl[8], and Clark J. Zeebregts[1]

[1]Department of Surgery, University Medical Centre Groningen, University of Groningen, Groningen, The Netherlands; [2]Department of Rheumatology and Clinical Immunology, University Medical Centre Groningen, University of Groningen, Groningen, The Netherlands; [3]Cardiovascular Medicine Section, Yale University School of Medicine, New Haven, Connecticut; [4]Department of Chemistry, Purdue University, Purdue, Indiana; [5]Department of Cardiology, University Medical Centre Groningen, University of Groningen, Groningen, The Netherlands; [6]Department of Nuclear Medicine and Molecular Imaging, University Medical Centre Groningen, University of Groningen, Groningen, The Netherlands; [7]Clinical Pharmacy and Pharmacology, University Medical Centre Groningen, University of Groningen, Groningen, The Netherlands; and [8]Department of Internal Medicine and Rheumatology, Martini Hospital, Groningen, The Netherlands

In atherosclerotic plaques, the risk of rupture is increased at sites of macrophage accumulation. Activated macrophages express folate receptor-β (FR-β), which can be targeted by folate coupled to radioactive ligands to visualize vulnerability. The aim of this study was to explore the presence of activated macrophages in human atherosclerotic plaques by ^{99m}Tc-folate imaging and to evaluate whether this technique can discriminate between an M1-like and M2-like macrophage phenotype. **Methods:** Carotid endarterectomy specimens of 20 patients were incubated with ^{99m}Tc-folate, imaged using micro-SPECT, and divided into 3-mm slices. The mean accumulation was calculated per slice, and the distribution of M1-like and M2-like macrophages per slice was quantified by immunohistochemical staining for CD86 as well as inducible nitric oxide synthase (iNOS) for M1 and CD163 and FR-β for M2 macrophages. Monocytes from healthy donors were differentiated toward M1-like or M2-like phenotype by in vitro culturing. Messenger RNA levels of specific M1 and M2 markers were measured by reverse-transcription polymerase chain reaction and expression of FR-β, CD86, and CD163 by flow cytometry. **Results:** There was a heterogeneous accumulation of ^{99m}Tc-folate in plaques (median, 2.45 [0.77–6.40] MBq/g). Slices with the highest ^{99m}Tc-folate accumulation of each plaque showed significantly more expression of FR-β and CD163, compared with slices with the lowest ^{99m}Tc-folate accumulation, which showed significantly more expression of iNOS. In in vitro polarized macrophages, messenger RNA expression of FR-β, mannose receptor, IL-10, and matrix metalloproteinase-9 was significantly increased in M2-like macrophages, compared with M1-like macrophages. On a receptor level, CD86 was shown to be overexpressed on M1-like macrophages whereas FR-β and CD163 were overexpressed on M2-like macrophages measured by flow cytometry. **Conclusion:** Higher numbers of M2-like macrophages were present in areas of high ^{99m}Tc-folate accumulation than areas with low accumulation. It is anticipated that ^{99m}Tc-folate imaging using SPECT as a marker for M2-like macrophages in atherosclerosis might be a good indicator for plaque vulnerability.

Received Jun. 16, 2014; revision accepted Sep. 4, 2014.
For correspondence or reprints contact: C.J. Zeebregts, Department of Surgery, Division of Vascular Surgery, University Medical Center Groningen, PB 30.001, 9700 RB Groningen, The Netherlands.
E-mail: czeebregts@hotmail.com
Published online Oct. 30, 2014.

Key Words: carotid artery; atherosclerotic plaque; vulnerability; folate receptor-β imaging; M2-like macrophages

J Nucl Med 2014; 55:1945–1951
DOI: 10.2967/jnumed.114.143180

Cardiovascular atherosclerotic disease is the main cause of death in the Western world (*1*). Clinical events such as myocardial infarction and ischemic cerebrovascular accident are directly related to the risk of atherosclerotic plaque rupture. Histologic analysis of a vulnerable plaque suggests the importance of necrotic core size; extent of inflammation; and angiogenesis, lipid accumulation, and fibrous cap thickness (*2*). Furthermore, in plaque vulnerability matrix metalloproteinases (MMPs), reactive oxygen species, inflammatory cytokines, and various growth factors released by activated macrophages play important roles (*3*). Patients with symptoms and carotid artery stenosis greater than 70% or those asymptomatic with carotid artery stenosis of 80%–90% are deemed suitable for endarterectomy, thereby significantly reducing the risk of subsequent major cerebrovascular accident or death (*4*). Imaging techniques currently used to visualize carotid artery stenosis include duplex ultrasound, CT angiography, and angiography (*5*). However, these techniques focus on anatomic features of the plaque and barely give any information on molecular and cellular processes. They therefore cannot distinguish between stable and unstable plaques. Because plaque composition rather than stenosis is important in detecting an unstable plaque, new imaging modalities are needed (*5*).

^{18}F-FDG PET can be used to identify vulnerable plaques in atherosclerotic disease, because ^{18}F-FDG accumulates in activated macrophages. ^{18}F-FDG micro-PET accumulation correlated well with macrophage content in a rabbit model, whereas in vivo quantification did not support this finding, possibly because of high accumulation in surrounding tissue (*6*). Folate receptor-β (FR-β) is present on activated macrophages but not on resting macrophages or other immune cells. For that reason, it might be a good indicator for inflammation in the human atherosclerotic carotid

plaque, as previously shown by imaging carotid artery specimens with fluorescence-labeled folate (*7*). Furthermore, Ayala-López et al. localized activated macrophages in apolipoprotein E (ApoE) knockout (KO) mice fed a western diet using a ^{99m}Tc-folate–labeled compound (*8*).

A heterogeneous population of macrophages exists including a classically activated macrophage type (M1) as well as an alternatively activated macrophage population (M2) (*9*). The M1 macrophage is thought to have proinflammatory properties, and polarization in vitro is driven by interferon γ and low-concentration lipopolysaccharide. Macrophages are driven toward the M2 type when the environment includes IL-4 and IL-10 (*10*). However, polarization of macrophages within a plaque is determined by the local microenvironment present in the atherosclerotic lesion and is thought to be rather more complex than the often used M1/M2 paradigm (*11*). As MMPs trigger plaque rupture, a M2-like macrophage type might be important as a direct cause of plaque vulnerability by producing tissue degrading MMPs (*12*).

Therefore, the major goal of this pilot study was to explore the distribution of macrophage subtypes in atherosclerotic plaques and the FR-β expression on the respective macrophage subtypes. In addition, the potential of technetium-labeled folate as a marker for atherosclerotic carotid plaque vulnerability was explored. To achieve this goal, the ^{99m}Tc-folate signal was compared with FR-β staining using specimens with a positive imaging ratio (accumulation slice/total plaque accumulation $>$ 1) to validate the folate–technetium compound. Additionally, macrophages were differentiated and polarized in vitro into M1-like and M2-like macrophages to investigate expression of FR-β and known M1 and M2 markers.

MATERIALS AND METHODS

Study Design

Between August 2011 and May 2012, 20 carotid specimens were obtained by means of carotid endarterectomy of the carotid bifurcation using standard techniques (*13*). Patients underwent open carotid surgery at the University Medical Center Groningen and were symptomatic (i.e., with a history of recent cerebrovascular accident, transient ischemic attack, or amaurosis fugax). They presented with a stenosis of the common carotid artery of 70%–99% as detected by duplex ultrasound. Additionally, asymptomatic patients with a stenosis of 80%–99%, found by routine control, were eligible for surgical treatment. Risk factors such as hyperlipidemia, hypertension, smoking status, obesity (body mass index), and diabetes mellitus were recorded. Hyperlipidemia and hypertension were defined as described before by our group (*7*). For validation of macrophage markers, 6 healthy volunteers were included without known cardiovascular disease or risk factors. The study was approved by the Institutional Review Board of the University Medical Center Groningen, and informed consent was obtained from all patients and healthy volunteers.

Carotid Endarterectomy Sample Collection and Time Path of Study

The carotid samples collected during carotid endarterectomy were immediately transported in a phosphate buffer on ice to the U-SPECT-II system (MILabs), with a mean transport time of 18 ± 6 min. The optimal incubation time and concentration of ^{99m}Tc-folate was determined. To validate the ^{99m}Tc-folate signal, immunohistochemistry was used for determining M1-like and M2-like macrophage levels in regions with high and low ^{99m}Tc-folate accumulation.

^{99m}Tc-Folate Labeling and Imaging of Plaque Using micro-SPECT

To determine the exact location in which the ^{99m}Tc-folate accumulation had taken place within the plaque, ex vivo imaging was performed.

TABLE 1
Baseline Characteristics and Risk Factors for Atherosclerosis

Characteristic	Patients (n = 20)
Men (%)	12 (60)
Age (y)	68 ± 8
Symptomatic (%)	18 (90)
Transient ischemic attack (%)	8 (40)
Cerebrovascular accident (%)	7 (35)
Amaurosis fugax (%)	3 (15)
Body mass index (kg/m^2)	27 ± 4
Smoking status (%)	10 (50)
>1 pack a day (%)	4 (20)
≤1 pack a day (%)	6 (30)
None, smoked in last 10 y (%)	3 (15)
Hypertension (%)	15 (75)
Controlled with single drug (%)	6 (30)
Controlled with 2 drugs, n (%)	5 (25)
Requires > 2 drugs or uncontrolled (%)	4 (20)
Systolic blood pressure (mm Hg)	138 ± 15
Diastolic blood pressure (mm Hg)	74 ± 8
Hyperlipidemia (%)	12 (60)
Use of lipid-lowering drugs (%)	17 (85)
Diabetes mellitus (%)	3 (15)*

*Two patients had diabetes controlled by diet or oral agents, and 1 patient was on insulin.

Data are mean ± SD, with percentages in parentheses.

A ^{99m}Tc-labeled imaging agent consisting of the vitamin folic acid conjugated to a chelating agent with specificity for ^{99m}Tc was used as follows: 1 mL of sodium pertechnetate ^{99m}Tc injection (100 MBq) was injected into a shielded vial. The vial was gently swirled for 30 s to dissolve the lyophilized powder and placed into a lead shield and incubated at 100°C for 18 min. Subsequently, the ^{99m}Tc-folate vial was cooled for 15 min protected from light, and the radiochemical

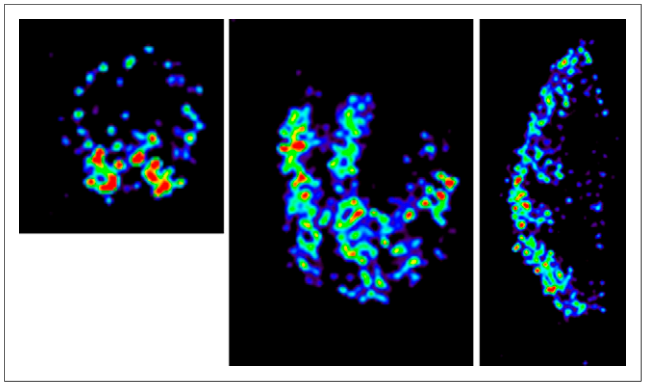

FIGURE 1. Transversal (left), coronal (middle), and sagittal (right) sections of micro-SPECT image of atherosclerotic carotid plaque specimen after ^{99m}Tc-folate incubation showing heterogeneous accumulation. Transversal image shows that area of higher accumulation (red) is confined within vessel wall.

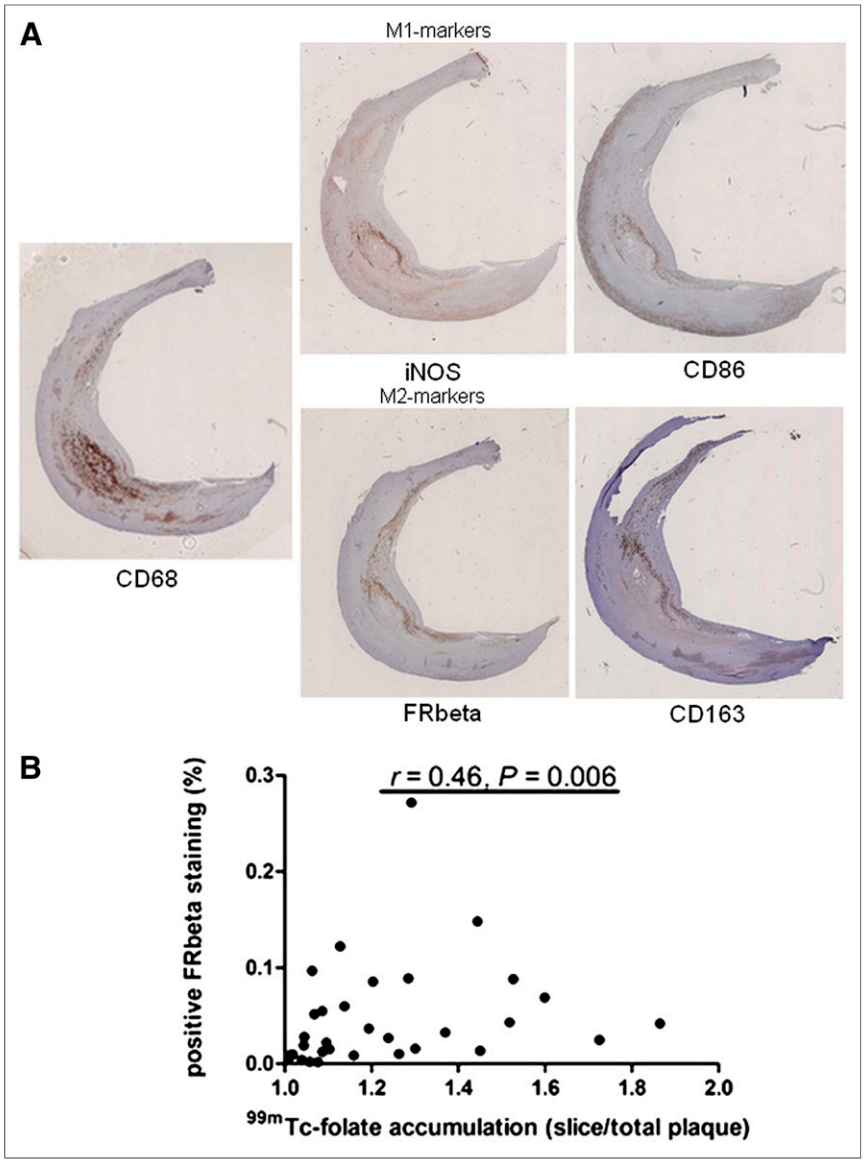

FIGURE 2. Immunohistochemical staining of 10 atherosclerotic plaques. (A) Staining of CD68, CD86, CD163, FR-β, and iNOS is depicted in slice with highest accumulation of ^{99m}Tc-folate in plaque. (B) Positive ^{99m}Tc-folate slices (accumulation slice/accumulation total plaque > 1) showed positive correlation with FR-β staining ($r = 0.46$, $P = 0.006$).

purity of ^{99m}Tc-folate was determined by instant thin-layer chromatography using saline as the eluent. The radiochemical purity must be greater than 90% to pass acceptance criteria. The carotid specimens were weighed and incubated for 1 h in 5 mL of a ^{99m}Tc-folate–containing solution at room temperature. After washing, ^{99m}Tc-folate accumulation was measured using the dose calibrator. The specimens were put into a micro-SPECT scanner, near the center of field of view, and scanned for 1 h (as determined by serial dilution). micro-SPECT images were corrected for scatter and reconstructed, applying an interactive reconstruction algorithm (2-dimensional ordered-subset expectation maximization). After incubation and scanning, all specimens were divided in equal slices of 3 mm. For every slice, the mean accumulation was calculated as counts/voxel of region of interest versus total dose calibrator activity per gram (total plaque weight), expressed as MBq/g. Images acquired were processed using AMIDE software (*14*).

Immunohistochemistry and Validation of ^{99m}Tc-Folate Signal

After determining ^{99m}Tc-folate accumulation of every slice, slices of plaques of 10 patients were embedded in paraffin, and sections of 4 μm were made. Macrophages were identified by incubation with monoclonal mouse antihuman CD68 (1:50; mo876 clone PG-M1; DAKO). For detection of M1 macrophages, rabbit antihuman inducible nitric oxide synthase (iNOS) and rabbit antihuman antibody CD86 (ab15323 and ab53004, respectively; Abcam) were used. To show M2-like macrophage distribution, mouse antihuman CD163 (a widely used M2 macrophage marker and mainly found in advanced human lesions near intraplaque hemorrhage areas (*15*); ab74604, [Abcam]) and biotinylated sheep antihuman FR-β antibody were used (BAF 5697; R&D Systems). Also, FR-β and CD163 were used for double staining to show colocalization of M2-like macrophages and FR-β expression. Appropriate secondary antibodies labeled with horseradish peroxidase and alkaline phosphatase for double staining were used. Color reaction was developed using 3, 3′-diaminobenzidine (DAKO) staining with chromogen (fast red [Sigma] for double staining with alkaline phosphatase), and sections were counterstained with hematoxylin. All sections were stored digitally after examination using a Nanozoomer Digital Pathology Scanner (NDP Scan U10074-01; Hamamatsu Photonics K.K.) and quantified (percentage of positive cells/total cells) with ImageScope Viewer software (V11.2.0.780 Aperio; e-Pathology Solution). For validation, slices with the lowest mean accumulation of the ^{99m}Tc-folate signal in imaging were compared with the slices with the highest mean accumulation in every carotid plaque separately (both compared with mean accumulation in the total plaque in counts/voxel).

In Vitro Differentiation and Polarization of M1-Like and M2-Like Macrophages

Peripheral blood mononuclear cells were isolated from 6 healthy donors by density gradient centrifugation using Lymphoprep (Axis Shield PoC As). Subsequently, monocytes were allowed to adhere to culture plates. The adherent cells were maintained for 5 d in RPMI 1640 medium (Lonza) supplemented with 10% filtered fetal calf serum. Macrophage colony-stimulating factor (20 ng/mL; R&D Systems) was added to the cell culture for differentiation into macrophages. Macrophages were directed toward M1-like and M2-like phenotypes by use of 48-h stimulation with interferon γ (100 U/mL; PeproTech) and lipopolysaccharide (1 ng/mL; Sigma) or IL-4 (20 ng/mL) and IL-10 (10 ng/mL) (PeproTech).

Flow Cytometry of M1-Like and M2-Like Macrophages

In vitro–differentiated M1-like and M2-like macrophages were stained with biotinylated antihuman FR-β antibody (R&D Systems) to explore protein expression. Streptavidine–allophycocyanine (Biolegend) was used as a secondary antibody. Anti-CD86-FITC

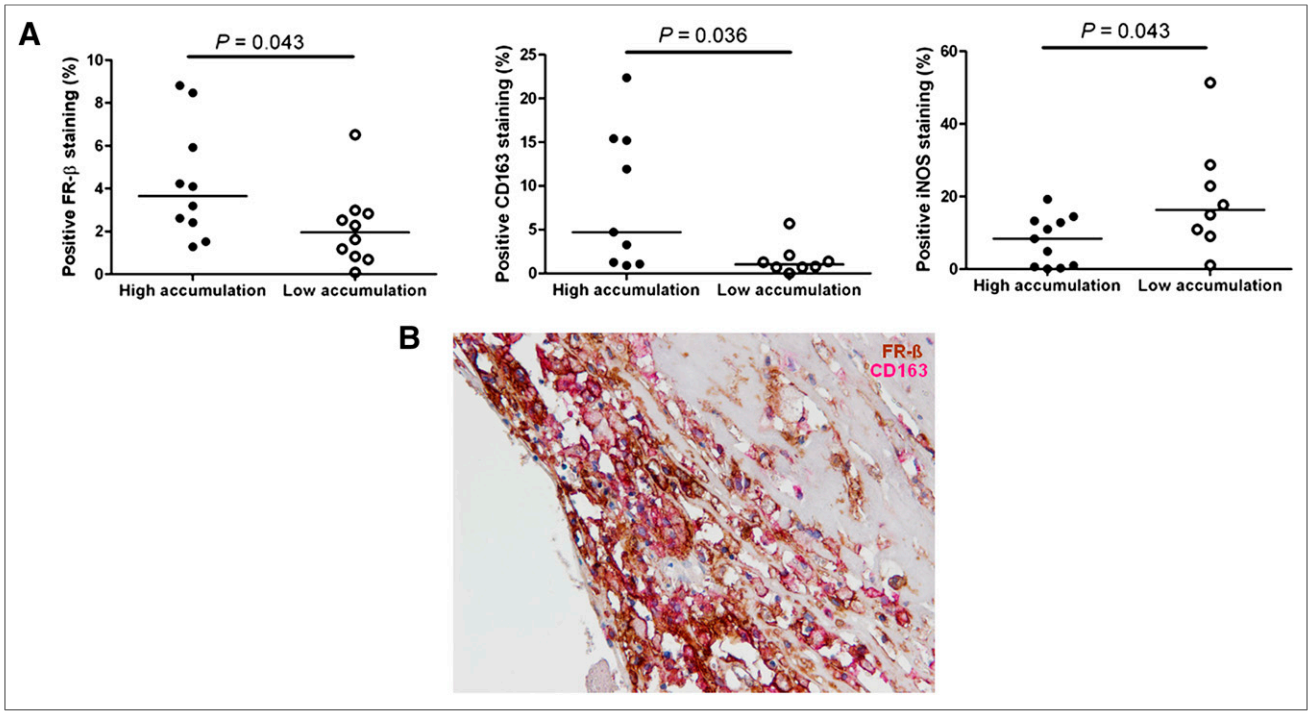

FIGURE 3. (A) Quantification of stainings. (A) Slices with highest ^{99m}Tc-folate accumulation (closed dots) showed significantly more FR-β expression than slices with lowest ^{99m}Tc-folate accumulation (open dots, $P = 0.043$) (left), slices with highest ^{99m}Tc-folate accumulation (closed dots) showed significantly more CD163 staining than slices with lowest ^{99m}Tc-folate accumulation (open dots, $P = 0.036$) (middle), and slices with lowest ^{99m}Tc-folate accumulation (open dots) showed significantly more iNOS staining than slices with highest ^{99m}Tc-folate accumulation (closed dots, $P = 0.043$) (right). (B) Double staining of CD163 and FR-β to show colocalization of M2-like macrophages and FR-β expression.

(fluorescein isothiocyanate) (BD Bioscience) and anti-CD163-PE (phycoerythrin) (Biolegend) were used to distinguish expression of these markers on macrophage subtypes. These were measured using flow cytometry.

RNA Isolation, Complementary DNA Synthesis, and Quantitative Reverse-Transcription Polymerase Chain Reaction

RNA was extracted from M1-like and M2-like macrophages as described before (*7*). For measurement of messenger RNA (mRNA), 1 μL of a complementary DNA sample was added in duplicate for amplification by the Taqman real-time PCR system (ABI Prism 7900HT Sequence Detection system; Applied Biosystems). Investigated genes were glyceraldehyde 3-phosphate dehydrogenase (GAPDH), IL-6, tumor necrosis factor (TNF), Tolllike receptor (TLR) 2 and 4, FR-β (folate receptor 2 or β), mannose receptor (CD206 or MR), IL-10, and MMP-9. Ct (threshold cycle) values were determined using the software program SDS 2.4 (Applied Biosystems). Relative gene expression was normalized to the expression of GAPDH and calculated by the following formula: relative gene expression = $2^{-\Delta Ct}$ (ΔCt = Ct gene of interest – Ct GAPDH).

Statistics

Values are presented as mean ± SD or median (with range in parentheses), unless stated otherwise. For correlations, Pearson and Spearman correlation coefficients were used when appropriate. A 2-tailed, paired Student *t* test was used for parametric distributions. Nonpaired continuous variables with a nonparametric distribution were analyzed using the Mann–Whitney *U* test. A 2-sided *P* value of less than 0.05 was considered statistically significant. Statistical tests were done with the Statistical Package for the Social Sciences (SPSS statistics version 20.0; SPSS Inc.).

RESULTS

Patient Characteristics

Twelve men and 8 women (mean age ± SD, 68.0 ± 8.4 y) were included. Patient characteristics are shown in Table 1.

Imaging of Plaque Using micro-SPECT

Imaging of 20 atherosclerotic plaques using micro-SPECT showed that ^{99m}Tc-folate accumulation occurred in specific areas of the plaques, with a median total activity of 2.45 (range, 0.77–6.40) MBq/g measured in a dose calibrator (Fig. 1). After scanning, all specimens were divided in equal slices, and ratio per slice was calculated (accumulation slice/total plaque accumulation). There were 5 ± 1 slices per atherosclerotic carotid plaque. ^{99m}Tc-folate accumulation was heterogeneously distributed throughout plaques (slices with highest ^{99m}Tc-folate ratio, 1.28 [1.03–2.24], and slices with the lowest ^{99m}Tc-folate ratio, 0.8 [0.18–0.99]).

Immunohistochemistry and Validation of ^{99m}Tc-Folate Signal

Plaque slices of 10 patients were stained using FR-β to validate the ^{99m}Tc-folate signal and also for CD68 (pan macrophages), CD86 and iNOS (M1 macrophage markers), and CD163 (M2 macrophage marker). In Figure 2A, representative staining is shown. All stainings were quantified with ImageScope software and expressed as percentage of positive cells per total cells. Slices with a positive ^{99m}Tc-folate imaging ratio (accumulation slice/total plaque accumulation > 1) were positively correlated to FR-β staining ($P = 0.006$, Fig. 2B). Figure 3 shows that FR-β staining in slices with the highest ^{99m}Tc-folate accumulation of each plaque was higher than in slices with the lowest accumulation ($P = 0.042$). The same was shown for CD163 staining ($P = 0.036$).

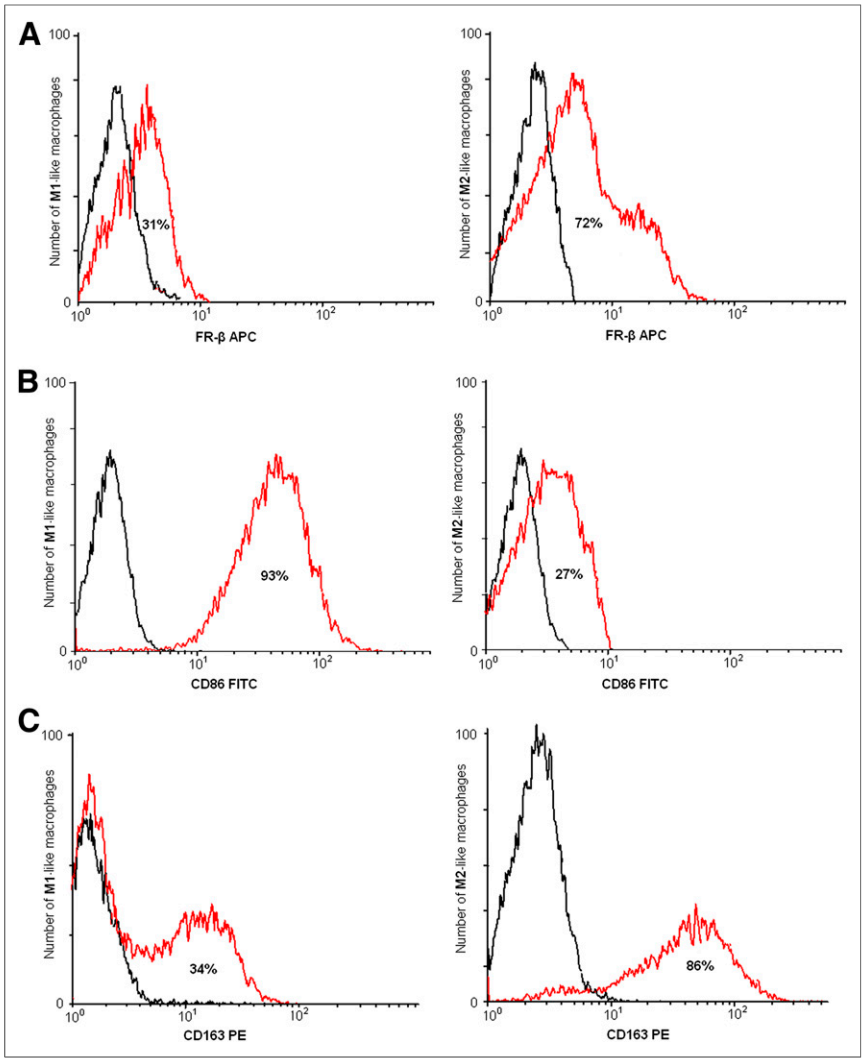

FIGURE 4. Representative flow cytometric analysis of M1-like and M2-like macrophage population from in vitro polarized macrophages, derived from peripheral blood mononuclear cells from healthy control. (A) FR-β is expressed on 31% of M1-like macrophages and on 72% of M2-like macrophages (red line). (B) CD86 is expressed on 93% of M1-like macrophages and on 27% of M2-like macrophages (red line). (C) CD163 is expressed on 34% on M1-like macrophages and on 86% of M2-like macrophages (red line). Isotypes in black in all graphs. APC = allophycocyanine; PE = phycoerythrin.

iNOS staining, on the contrary, showed a significantly higher percentage of positive cells in the slices with lowest accumulation of ^{99m}Tc-folate than with the highest accumulation ($P = 0.043$). However, staining of CD68 and CD86 was not significantly different in slices with the highest accumulation of ^{99m}Tc-folate, compared with slices with lowest accumulation ($P = 0.43$ and 0.44, respectively). Furthermore, CD163 colocalized with FR-β expression in a carotid plaque, as can be seen in a representative picture (Fig. 3B).

Expression of Macrophage Markers by Flow Cytometry

To validate FR-β, CD86, and CD163 as macrophage subtype markers, their expression on macrophage subpopulations was determined using flow cytometry (representative examples in Fig. 4). FR-β is expressed on 31% of M1-like macrophages and on 72% of M2-like macrophages. In M1-like macrophages, 93% (60–97) of cells were positive for CD86, whereas 34% (5–45) of cells were positive for CD163. In contrast, M2-like macrophages showed a high expression of CD163 (86% [56–95]) whereas CD86 expression was lower (27% [10–40]), both measured in 10 healthy volunteers.

In Vitro mRNA Expression of M1-Like and M2-Like Markers

mRNA levels of GAPDH, IL-6, TNF, TLR-2 and -4, FR-β, MR, IL-10, and MMP-9 were determined in M1-like and M2-like differentiated macrophages in duplicate from 6 healthy volunteers. The mRNA expression of FR-β, MR, IL-10, and MMP-9 was increased in M2-like macrophages, compared with M1-like macrophages ($P = 0.09$, 0.04, 0.06, and 0.004, respectively, Fig. 5). On the contrary, TNF and TLR-2 mRNA levels were significantly higher in M1-like macrophages than in M2-like macrophages (Fig. 6, $P = 0.002$ for both). No significant difference could be found in mRNA levels of IL-6 and TLR-4 between M1-like and M2-like macrophages.

DISCUSSION

This is the first study, to our knowledge, to show feasibility using ^{99m}Tc-folate to image human atherosclerotic carotid plaques ex vivo. Slices with the highest ^{99m}Tc-folate accumulation showed significantly more FR-β and CD163 expression, compared with slices with the lowest ^{99m}Tc-folate accumulation, and significantly less expression of iNOS. Therefore, FR-β–positive macrophages were found to be primarily M2-like polarized macrophages, which might be proatherogenic, due to production of matrix-degrading enzymes.

Several research groups succeeded in specifying macrophage subsets expressing the folate receptor on tumor-associated M2 macrophages (*16*) and on M2 macrophages expressed in experimental allergic asthma in mice (*17*). Furthermore, FR-β–targeted immunotoxin treatment resulted in the reduction of macrophages and plaque progression (*18*). However, by our knowledge this is also the first study to show an overexpression of FR-β on M2-like macrophages in atherosclerosis. Nevertheless, identification of macrophage subtypes and determination of their role in the atherosclerotic process is still a major challenge.

The M1 and M2 macrophage subtypes were observed in atherosclerotic lesions previously (*19,20*). Shaikh et al. found a higher proportion of M1 proinflammatory macrophages and a reduced proportion of M2 cells in symptomatic carotid lesions (*21*). The discrepancy to our study could be due to the fact that the former study compared the ratio of macrophage subtypes in the carotid artery with those in vascular femoral plaques. In an experimental atherosclerotic ApoE KO mice model, lesion progression was correlated with the dominance of M1 (arginase [Arg] II$^+$) over the M2 (Arg I$^+$) macrophage subtype (*22*). This result could

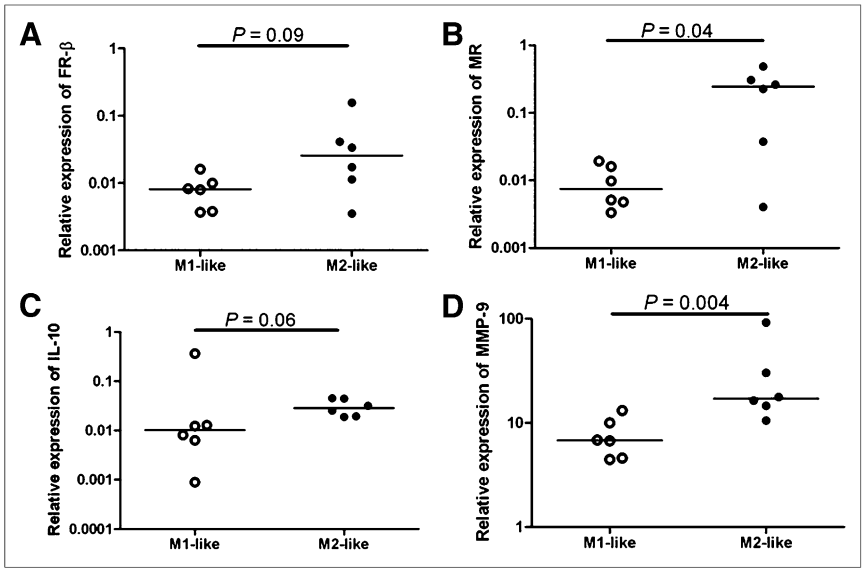

FIGURE 5. Relative expression of mRNA levels to GAPDH in 6 healthy volunteers. Quantitative reverse-transcription polymerase chain reaction revealed higher relative expression in M2-like macrophages (black dots) than M1-like macrophages (open dots) in FR-β ($P = 0.09$) (A), MR ($P = 0.04$) (B), IL-10 ($P = 0.06$) (C), and MMP-9 ($P = 0.004$) (D).

be due to the proportion of M1 and M2 macrophages depending on stadium of plaque formation in the ApoE model. In recent published studies, other M2 markers were found to be related to worse cardiovascular outcome (*23–26*). In sections derived from subjects enrolled in the Cardiovascular Pathology Institute Sudden Coronary Death Registry, stable plaques revealed few M2-like macrophages (made visible by targeting the MR), compared with unstable plaques in which the M2-like macrophage subpopulation was abundant (*23*). Furthermore, patients with a 2.4-fold increased cardiovascular risk, compared with patients with a low ratio, were found to have a high MMP-12/CD68 ratio (*24*). MMP-12 was found to be correlated with MMP-9–positive macrophage subpopulations in a mouse model for obesity (*25*). Stöger et al. found a correlation between areas of intraplaque hemorrhage and CD163 staining in human atherosclerosis. During development of plaques both M1 and M2 cells accumulated, and the fibrous caps of lesions showed no significant differences between subsets. In contrast, vascular adventitial tissue displayed a pronounced M2 activation profile (*26*). These different studies support our hypothesis that accumulation of M2-like macrophages might be indicative of plaque vulnerability, which can be imaged by ^{99m}Tc-folate.

Folate receptors have been visualized before using optical fluorescent contrast agent (FITC) labeled to folate by our group (*7*). Other groups also used optical imaging for the identification of tumor processes, as several solid tumors express folate receptor-α, demonstrated in ovarian cancer (*27*) and in head and neck carcinoma expressing FR-β (*28*). However, applications for noninvasive optical imaging of fluorescent signals by the use of fluorophores such as FITC could be of less clinical value because of the limited penetration depth of only a few millimeters. This small penetration depth could be extended to a few centimeters using near-infrared probes, but these are not ideal for use in, for example, coronary arteries. ^{99m}Tc-folate has a good tissue penetration and a relatively short half-life. Furthermore, the radiolabeling procedure for ^{99m}Tc-folate is simple, and it has not shown toxicity or immunogenicity (*8*).

For in vivo folate receptor imaging, the SPECT modality could be used; Ayala Lopez et al. tested ^{99m}Tc-folate accumulation in ApoE KO mice on a Western chow diet and showed a significantly greater accumulation in atherosclerotic lesions than in mice on normal chow (*8*). In humans, ^{111}In-DTPA-folate and ^{99m}Tc-EC20-folate have been tested in clinical trials as radiotracers for imaging of cancer (FR-α) (*29,30*). Nevertheless, Winkel et al. showed that ^{111}In-EC0800 (a radiolabeled folate compound) detects plaque but was not able to differentiate between a stable and a vulnerable atherosclerotic carotid plaque in a shear stress-induced ApoE KO mouse model (*31*). However, in this model macrophage content is not different between the oscillatory shear stress region (stable plaque) and the lowered shear stress region (vulnerable plaque) (*32*). Also PET tracers have been developed recently, of which 3′-aza-2′-^{18}F-fluorofolic acid (*33*) has been shown to selectively target FR-β–positive macrophages in atherosclerotic plaques (*34*). No determination of differential folate accumulation in the respective M1-like and M2-like subpopulation was performed in this study. ^{18}F-fluoro-polyethylene glycol-folate has been used in a rat model of arthritis to image subclinical arthritis (*35*). For imaging of plaque inflammation, 2-deoxy-2-^{18}F-fluoro-D-mannose has been developed recently, supporting a higher accumulation in macrophages than ^{18}F-FDG (*23*).

A limitation of our study is that division of macrophages solely as M1 or M2 subtypes may be too simple. As Wolfs et al. suggest, the role of the local microenvironment makes macrophage polarization in the atherosclerotic tissue more complex than the typically described M1 and M2 macrophages distribution (*11*). Thus, not only cytokine environment but also foam cell formation and CXCL4 (chemokine ligand 4, forming M4 macrophages), among other factors, play major roles. The presence of other macrophages could explain why a CD68+ population in the plaque does not stain for M1/M2 markers or FR-β

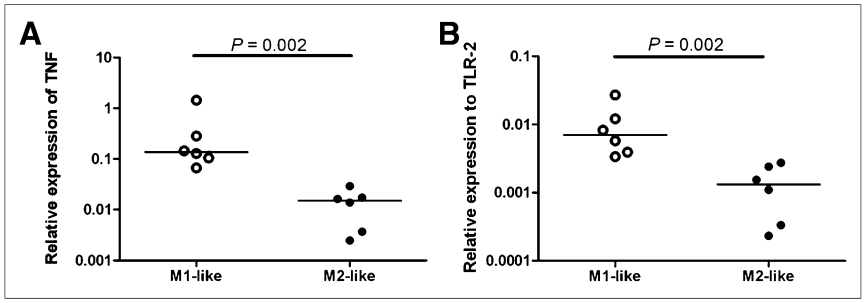

FIGURE 6. Relative expression of mRNA levels to GAPDH in 6 healthy volunteers measured in duplo showing higher relative expression in M1-like macrophages (open dots) than M2-like macrophages (black dots) in TNF ($P = 0.002$) (A) and TLR-2 ($P = 0.002$) (B).

(Fig. 2A). Further studies to investigate the release of MMPs by macrophage subtypes may give more insight. Also, because of the inclusion of a low number of asymptomatic patients, no analyses between the ratio of M1-like and M2-like macrophages in symptomatic and asymptomatic disease could be made. More research is necessary to explore this issue.

CONCLUSION

This is the first study showing a positive correlation between accumulation of a ^{99m}Tc-folate compound in atherosclerotic plaques and FR-β expression on M2-like macrophages. Furthermore, we characterized macrophage phenotypes ex vivo and in vitro by a panel of macrophage subtype markers. This characterization of macrophage phenotypes not only enables the specific analysis of the proportion of macrophage subtypes within a plaque, but also opens ways to measure M2-like macrophage populations ex vivo. More insight into macrophage subtypes and behavior in atherosclerotic plaques may give a better understanding of the pathogenesis related to the vulnerability of atherosclerotic plaques.

DISCLOSURE

The costs of publication of this article were defrayed in part by the payment of page charges. Therefore, and solely to indicate this fact, this article is hereby marked "advertisement" in accordance with 18 USC section 1734. No potential conflict of interest relevant to this article was reported.

ACKNOWLEDGMENTS

We thank Fleur Schaper, Gerda Horst, and Gerda de Vries for measuring macrophage markers using flow cytometry; Irene Zwarts for measuring macrophage markers using RT-PCR; and Berber Doornbos for performing immunohistochemical stainings.

REFERENCES

1. World Health Organization. The top 10 causes of death. Fact sheet no. 31. World Health Organization website. http://www.who.int/mediacentre/factsheets/fs310/en/index.html. 2011. Accessed August 27, 2014.
2. Finn AV, Nakano M, Narula J, Kolodgie FD, Virmani R. Concept of vulnerable/unstable plaque. *Arterioscler Thromb Vasc Biol.* 2010;30:1282–1292.
3. Libby P, Ridker PM, Hansson GK. Progress and challenges in translating the biology of atherosclerosis. *Nature.* 2011;473:317–325.
4. Zeebregts CJ, Meerwaldt R, Geelkerken RH. Carotid artery stenting: a 2009 update. *Curr Opin Cardiol.* 2009;24:528–531.
5. Hermus L, van Dam GM, Zeebregts CJ. Advanced carotid plaque imaging. *Eur J Vasc Endovasc Surg.* 2010;39:125–133.
6. Masteling MG, Zeebregts CJ, Tio RA, et al. High-resolution imaging of human atherosclerotic carotid plaques with micro ^{18}F-FDG PET scanning exploring plaque vulnerability. *J Nucl Cardiol.* 2011;18:1066–1075.
7. Jager NA, Westra J, van Dam GM, et al. Targeted folate receptor β fluorescence imaging as a measure of inflammation to estimate vulnerability within human atherosclerotic carotid plaque. *J Nucl Med.* 2012;53:1222–1229.
8. Ayala-López W, Xia W, Varghese B, Low PS. Imaging of atherosclerosis in apoliprotein e knockout mice: targeting of a folate-conjugated radiopharmaceutical to activated macrophages. *J Nucl Med.* 2010;51:768–774.
9. Medbury HJ, James V, Ngo J, et al. Differing association of macrophage subsets with atherosclerotic plaque stability. *Int Angiol.* 2013;32:74–84.
10. Jager NA, Teteloshvili N, Zeebregts CJ, Westra J, Bijl M. Macrophage folate receptor β (FR-β) expression in auto-immune inflammatory rheumatic diseases: a forthcoming marker for cardiovascular risk? *Autoimmun Rev.* 2012;11:621–626.
11. Wolfs IM, Donners MM, de Winther MP. Differentiation factors and cytokines in the atherosclerotic plaque micro-environment as a trigger for macrophage polarisation. *Thromb Haemost.* 2011;106:763–771.
12. Mantovani A, Sica A, Sozzani S, Allavena P, Vecchi A, Locati M. The chemokine system in diverse forms of macrophage activation and polarization. *Trends Immunol.* 2004;25:677–686.
13. Meerwaldt R, Hermus L, Reijnen MM, Zeebregts CJ. Carotid endarterectomy: current consensus and controversies. *Surg Technol Int.* 2010;20:283–291.
14. Loening AM, Gambhir SS. AMIDE: A free software tool for multimodality medical image analysis. *Mol Imaging.* 2003;2:131–137.
15. Boyle JJ, Harrington HA, Piper E, et al. Coronary intraplaque hemorrhage evokes a novel atheroprotective macrophage phenotype. *Am J Pathol.* 2009;174:1097–1108.
16. Puig-Kröger A, Sierra-Filardi E, Dominguez-Soto A, et al. Folate receptor beta is expressed by tumor-associated macrophages and constitutes a marker for M2 anti-inflammatory/regulatory macrophages. *Cancer Res.* 2009;69:9395–9403.
17. Shen J, Chelvam V, Cresswell G, Low PS. Use of folate-conjugated imaging agents to target alternatively activated macrophages in a murine model of asthma. *Mol Pharm.* 2013;10:1918–1927.
18. Furusho Y, Miyata M, Matsuyama T, et al. Novel therapy for atherosclerosis using recombinant immunotoxin against folate receptor beta-expressing macrophages. *J Am Heart Assoc.* 2012;1:e003079.
19. Bouhlel MA, Derudas B, Rigamonti E, et al. PPARgamma activation primes human monocytes into alternative M2 macrophages with anti-inflammatory properties. *Cell Metab.* 2007;6:137–143.
20. Finn AV, Nakano M, Polavarapu R, et al. Hemoglobin directs macrophage differentiation and prevents foam cell formation in human atherosclerotic plaques. *J Am Coll Cardiol.* 2012;59:166–177.
21. Shaikh S, Brittenden J, Lahiri R, Brown PA, Thies F, Wilson HM. Macrophage subtypes in symptomatic carotid artery and femoral artery plaques. *Eur J Vasc Endovasc Surg.* 2012;44:491–497.
22. Khallou-Laschet J, Varthaman A, Fornasa G, et al. Macrophage plasticity in experimental atherosclerosis. *PLoS ONE.* 2010;5:e8852.
23. Tahara N, Mukherjee J, de Haas HJ, et al. 2-deoxy-2-[^{18}F]fluoro-d-mannose positron emission tomography imaging in atherosclerosis. *Nat Med.* 2014;20:215–219.
24. Scholtes VP, Johnson JL, Jenkins N, et al. Carotid atherosclerotic plaque matrix metalloproteinase-12-positive macrophage subpopulation predicts adverse outcome after endarterectomy. *J Am Heart Assoc.* 2012;1:e001040.
25. Shaul ME, Bennett G, Strissel KJ, Greenberg AS, Obin MS. Dynamic, M2-like remodeling phenotypes of CD11c+ adipose tissue macrophages during high-fat diet–induced obesity in mice. *Diabetes.* 2010;59:1171–1181.
26. Stöger JL, Gijbels MJ, van der Velden S, et al. Distribution of macrophage polarization markers in human atherosclerosis. *Atherosclerosis.* 2012;225:461–468.
27. van Dam GM, Themelis G, Crane LM, et al. Intraoperative tumor-specific fluorescence imaging in ovarian cancer by folate receptor-alpha targeting: first in-human results. *Nat Med.* 2011;17:1315–1319.
28. Sun JY, Shen J, Thibodeaux J, et al. In vivo optical imaging of folate receptor-beta in head and neck squamous cell carcinoma. *Laryngoscope.* 2014;124:E312–E319.
29. Fisher RE, Siegel BA, Edell SL, et al. Exploratory study of ^{99m}Tc-EC20 imaging for identifying patients with folate receptor-positive solid tumors. *J Nucl Med.* 2008;49:899–906.
30. Edelman MJ, Harb WA, Pal SE, et al. Multicenter trial of EC145 in advanced, folate-receptor positive adenocarcinoma of the lung. *J Thorac Oncol.* 2012;7:1618–1621.
31. Winkel LC, Groen HC, van Thiel BS, et al. Folate receptor-targeted single-photon emission computed tomography/computed tomography to detect activated macrophages in atherosclerosis: can it distinguish vulnerable from stable atherosclerotic plaques? *Mol Imaging.* 2013;12:1–5.
32. Cheng C, Tempel D, van Haperen R, et al. Atherosclerotic lesion size and vulnerability are determined by patterns of fluid shear stress. *Circulation.* 2006;113:2744–2753.
33. Betzel T, Muller C, Groehn V, et al. Radiosynthesis and preclinical evaluation of 3′-aza-2'-[^{18}F]fluorofolic acid: a novel PET radiotracer for folate receptor targeting. *Bioconjug Chem.* 2013;24:205–214.
34. Müller A, Beck K, Rancic Z, et al. Imaging atherosclerotic plaque inflammation via folate receptor targeting using a novel ^{18}F-folate radiotracer. *Mol Imaging.* 2014;13:1–11.
35. Gent YY, Weijers K, Molthoff CF, et al. Evaluation of the novel folate receptor ligand [^{18}F]fluoro-PEG-folate for macrophage targeting in a rat model of arthritis. *Arthritis Res Ther.* 2013;15:R37.

JNM The Journal of NUCLEAR MEDICINE

Folate Receptor-β Imaging Using ^{99m}Tc-Folate to Explore Distribution of Polarized Macrophage Populations in Human Atherosclerotic Plaque

Nynke A. Jager, Johanna Westra, Reza Golestani, Gooitzen M. van Dam, Philip S. Low, René A. Tio, Riemer H.J.A. Slart, Hendrikus H. Boersma, Marc Bijl and Clark J. Zeebregts

J Nucl Med. 2014;55:1945-1951.
Published online: October 30, 2014.
Doi: 10.2967/jnumed.114.143180

The Journal of Nuclear Medicine is published monthly.
SNMMI | Society of Nuclear Medicine and Molecular Imaging
1850 Samuel Morse Drive, Reston, VA 20190.
(Print ISSN: 0161-5505, Online ISSN: 2159-662X)

SNMMI SOCIETY OF NUCLEAR MEDICINE AND MOLECULAR IMAGING